LiFePO$_4$ Crystal Growth during Co-precipitation

Chaochao Huang[1], Desheng Ai[1,3], Li Wang[1,4,*], Xiangming He[1,2,*]

[1] Institute of Nuclear & New Energy Technology, Tsinghua University, Beijing, 100084, China
[2] State Key Laboratory of Automotive Safety and Energy, Tsinghua University, Beijing 100084, China
[3] Beijing Key Laboratory of Fine Ceramics, Tsinghua University, Beijing 100084, PR China
[4] Huadong Institute of Lithium Ion Battery, Zhangjiagang, Jiangsu 215600, China
[*]E-mail: wang-l@tsinghua.edu.cn, hexm@tsinghua.edu.cn

Uniform LiFePO$_4$ nanoplates with an average thickness of 30 nm were synthesized within 15 min by co-precipitation at 180°C. The strong relevance among defect concentration, crystalline size and reactant concentration was investigated. The crystalline formation, as well as crystal growth, of LiFePO$_4$ is confirmed to be a three-dimensional diffusion-controlled process.

1. INTRODUCTION

Lithium iron phosphate (LiFePO$_4$) has been intensively investigated as a very promising cathode material for rechargeable lithium-ion batteries, because of its good cycling performance, good safety performance, low-cost raw material and non-toxicity.[1] However, the poor conductivity of both electron and Li$^+$ hinders the application of LiFePO$_4$. Since Li$^+$ ions diffusion in orthorhombic LiFePO$_4$ typically occurs along one-dimensional (1D) channels parallel to [020] direction, the delithiation and lithiation process in LiFePO$_4$ will be easily impeded by the presence of immobile and low-mobility defects residing in the diffusion path.[1-3] Theoretical calculation shows that Fe^{2+} on Li$^+$ sites (Fe$_{Li}^+$ antisite defect, and the percentage of this defect in the whole crystal is called disorder degree) is expected to be comparatively immobile in the 1D channels, which results in the poor conductivity of LiFePO$_4$.[2,3] Nanocrystallization and morphology control can reduce the disorder degree's negative influence on diffusion. Carbon coating can help improve the ionic/electronic conductivity of LiFePO$_4$.[4]

The typical disorder degree in solid-state synthesis (synthesis temperature 800-1100 K) is 0.1-0.5%. Though solid-state synthesis routes can obtain nano-size spherical $LiFePO_4$ with low disorder $LiFePO_4$, it can hardly control the morphology which may benefit the delithiation and lithiation process further.[2,3] Besides, high temperature is an indispensable factor in solid-state synthesis routes, which not only increases the energy consumption during synthesis, but also goes against the continuous manner. The carbon emission during lithium battery's whole cycle life (synthesis, battery assembly and reclamation) is about 72 kg/kWh.[5] It is difficult to manage down the energy demand for solid-state synthesis. A promising method is hydrothermal/solvothermal synthesis routes as its incomparable advantages in size and morphology control within a synthesis temperature far below the solid-state synthesis routes (about 400-500 K), which will really reduce the energy consumption and costs.[4,6] Traditional hydrothermal/solvothermal synthesis routes is performed in various autoclave within solvent water or organic solvents. Previous studies have proof that $LiFePO_4$ synthesized by hydrothermal method shows homogeneous particle size distribution, fast reaction rate and facile size control.[6-8] Introducing ethylene glycol as solvents into the reaction system resulted in a remarkable improvement of electrochemical properties.[9] As the boiling point of ethylene glycol is $197.3\,^{o}C$ and the suitable reaction temperature for hydrothermal/solvothermal synthesis routes is around $180\,^{o}C$, the autoclave may be not irreplaceable and is replaced with a reflux device.[9,10] The difference between hydrothermal/solvothermal synthesis routes and reflux method is pressure. With simple synthesis device, the reflux method promises a potential way to mass continuous production of nano-size $LiFePO_4$. As hydrothermal/solvothermal synthesized $LiFePO_4$ obtain a disorder about 3-8%, the crystal growth and defects motion in this routes should be carefully invesitaged.[11-13]

2. EXPERIMENT

In this work, all the chemicals (AR) were purchased from Sinopharm Chemical Reagent. In a typical synthesis, $LiOH \cdot H_2O$, $FeSO_4 \cdot 7H_2O$ and H_3PO_4 were used as the starting materials in a molar ratio of 2.7:1:1[14] while the ethylene glycol was used as the solvent. The reaction was performed in a reflux device. Firstly, 0.162 mol of $LiOH \cdot H_2O$ was dissolved in 200 mL of ethylene glycol under stirring to obtain LiOH solution in the reflux device. Subsequently, 0.06 mol of H_3PO_4 and $FeSO_4 \cdot 7H_2O$ were dissolved in 100 mL ethylene glycol under magnetic stirring. The mixed solution was slowly added to the above LiOH solution in the reflux device.[15] The mixed solution was stirred for 15 min and then heated up to $180\,^{o}C$ for 720 min in the reflux device with nitrogen and atmospheric pressure (without any stirring). The obtained gray precipitates were washed with deionized water and ethanol and drying for 6 hours at $60\,^{o}C$. There were 3 groups of reaction concentrations performed in this work with 18 sampling time points as shown as follows. Group a: 0.1mol/L (Fe^{2+} ion concentration); Group b: 0.2mol/L (Fe^{2+} ion concentration); Group c: 0.4mol/L (Fe^{2+} ion concentration). The Sampling time points were 0, 10, 20, 30, 40, 50, 60, 80, 100, 120, 150, 180, 210, 240, 360, 480, 600, 720 min, respectively.

The phase and crystal defects of the samples were identified by X-ray diffraction (XRD; Burker AXS D8 ADVANCE XRD Cu Kα radiation λ=1.5406Å). Morphologic studies were performed

by scanning electron microscopy (SEM; JEOL JSM-7100F FESEM) and transmission electron microscopy (TEM; JEOL JEM 201 & FEI Tecnai G^2 20).

3. RESULTS & DISCUSSION

Figure 1 shows the scanning electron microscope (SEM) images of the samples in different groups. The XRD pattern highly coincides with a lithium iron phosphate standard PDF card (space group Pnma, JCPDS Card No: 83-2092). It confirms that most specimens subjected to a reaction are pure and well-crystallized without any impurity phase, except for the samples produced by groups A and B under a 0 min reaction (just as the reaction device reaches 180 °C). These samples are in an amorphous state. In addition, no shaped crystal can be seen in the scanning electron micrograph, confirming the XRD result, but considerably differing from the later-crystallographic lithium iron phosphate. If reaction time lasts for 10 min or longer, the products generated are all LiFePO$_4$ nanoplates. The crystal produced by group C grows faster than those generated by groups A and B, and forms LiFePO$_4$ nanoplates in 0 min. In the same group, LiFePO$_4$ nanoplates at different reaction time have similar sizes, also indicating that its three-dimensional size in unrelated to reaction time. From some LiFePO$_4$ nanoplates, we can see that thickness is about 30 nm.

Comparing the sizes of the samples of different groups (crystal width), we can see the size of nameplates decrease when reaction concentration goes higher. The average size of the surface of LiFePO$_4$ in group A is 400 nm × 250 nm, whereas that in group C with a high concentration is only 200 nm × 100 nm. Within more nucleation core and higher diffusion speed at high concentration, nanoplates grow faster with smaller sizes.[15]
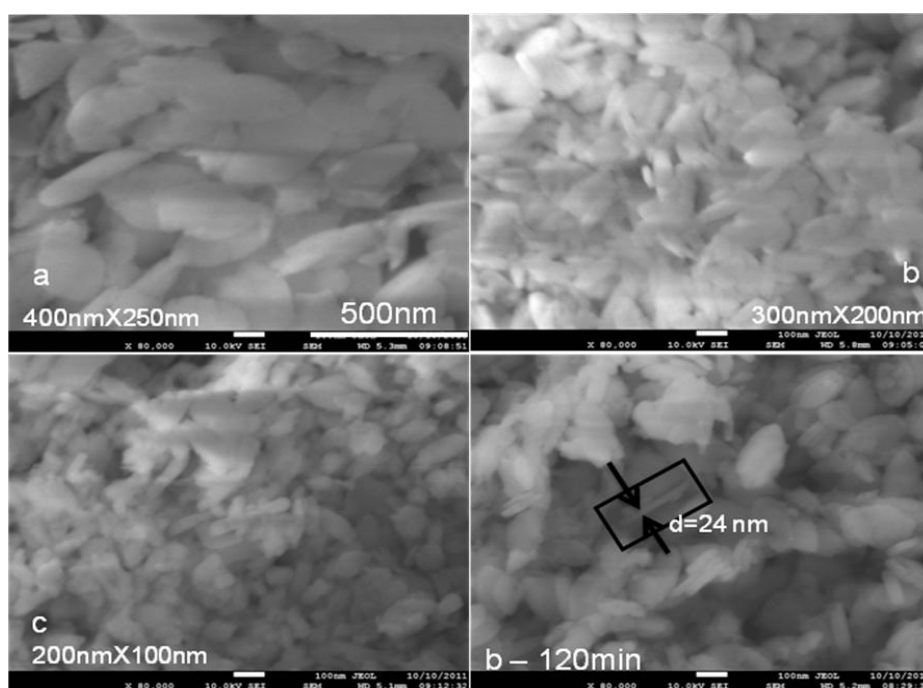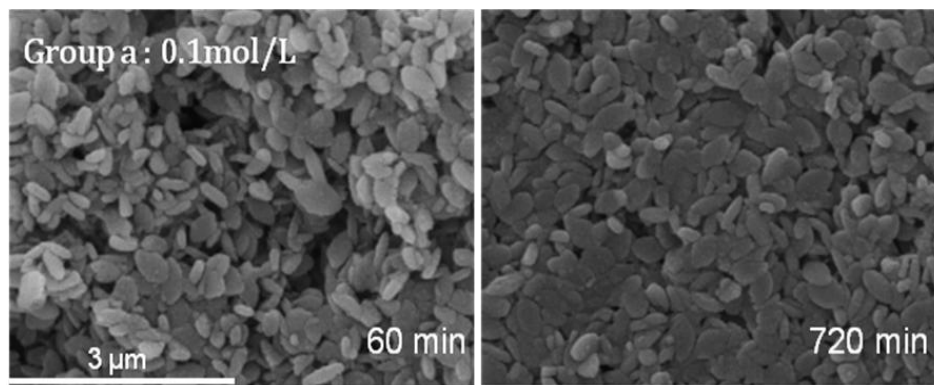
*Group a: sample time 60 min Vs 720 min. Almost the same size
**Group b&c share the same changes as showing in Group a, the size of nameplates did not change over time

Figure 1. XRD&SEM of Group a, b and c.

To confirm the plane of LiFePO$_4$ nanoplates, transmission electron microscopy (TEM) analysis of those nanoplates is induced. Figure 2 shows a representative TEM image of LiFePO4 nameplates. The selected-area electron diffraction (SAED) results indicate that the LiFePO$_4$ nanoplates exposed the (020) plane which is perpendicular to the (001) and (100) plane.[14,15]

A special XRD test also confirms the SAED results. The JCPDS card 83-2092 shows that the diffraction peak at 17.1^o stands for the (200) plane, 20.7^o stands for the (101) plane, 25.5^o stands for the (111/201) plane and 29.8^o stands for the (020/211) plane. When preparing the XRD samples in a different way, it will lead to different diffraction intensities for the 4 peaks. If the XRD sample is prepared by dispersing the nanoplates powder in anhydrous ethanol and then slowly drying on the glass sample stage, the peak intensity at 29.8^o will increase while the other 3 peaks' intensity (17.1^o, 20.7^o, 25.5^o) would decrease, comparing with the untreated sample (Figure 3). The untreated sample is random arranged, that means the nanoplates in which are chaotic and can form any angle to the sample stage, horizontal or vertical. While the other sample preparing by slowly drying, could be more regular and the number of the nanoplates parallel to sample stage's surface increased. As the (200), (101) and (201) planes are perpendicular to (020) plane, the intensity's decrease in slowly drying sample is obvious while the (020) peak increased.[14] This result agrees well with the SAED pattern.

The TEM and XRD results indicate that the LiFePO$_4$ nanoplates obtained by reflux method exhibits the same thickness direction along the b axis in terms of crystallography ([020] direction); the [020] direction is merely the diffusion path of lithium ion in LiFePO$_4$.[7] The nanoplates have an average thickness of 30 nm, which is favorable for the insertion and abjection of lithium ion, thereby increasing the ionic conductance of LiFePO$_4$.[7]

As the solvent, ethylene glycol plays a critical role in reflux method. By virtue of its high stickiness and unique molecular structure, it can preferentially absorb on the surface of (020) plane to prevent the crystal from growing in the [020] direction and leads to LiFePO$_4$ nanoplates with small-sized along the b axis.[10] In addition, ethylene glycol acts as a weak reductive agent in preventing Fe^{2+} from being oxidized.[10]
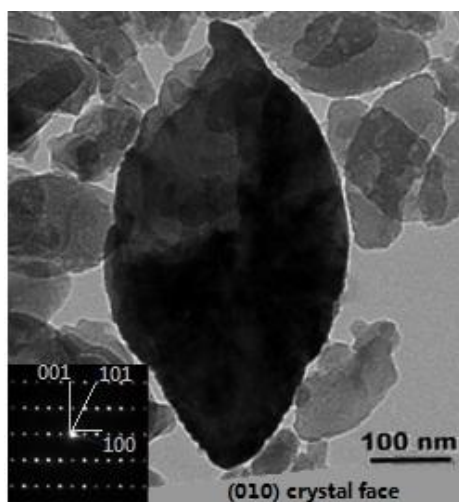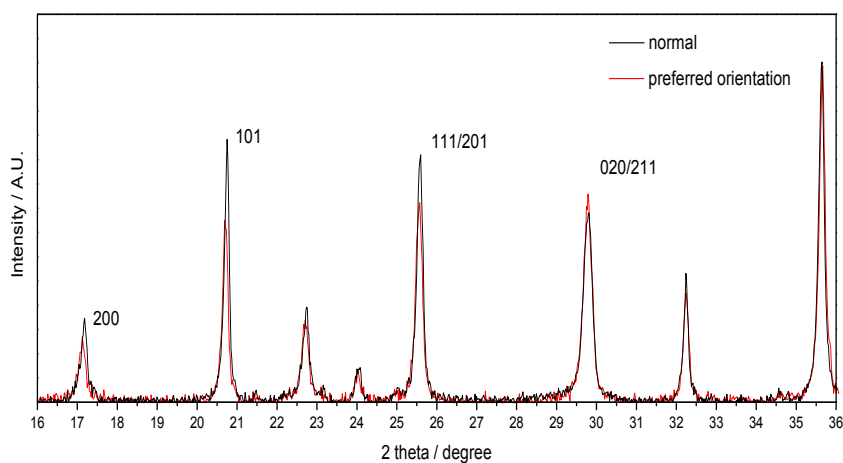
Figure 2. TEM of Group a: 60 min

Figure 3. XRD patterns of LiFePO4 nanoplates with different arrangement
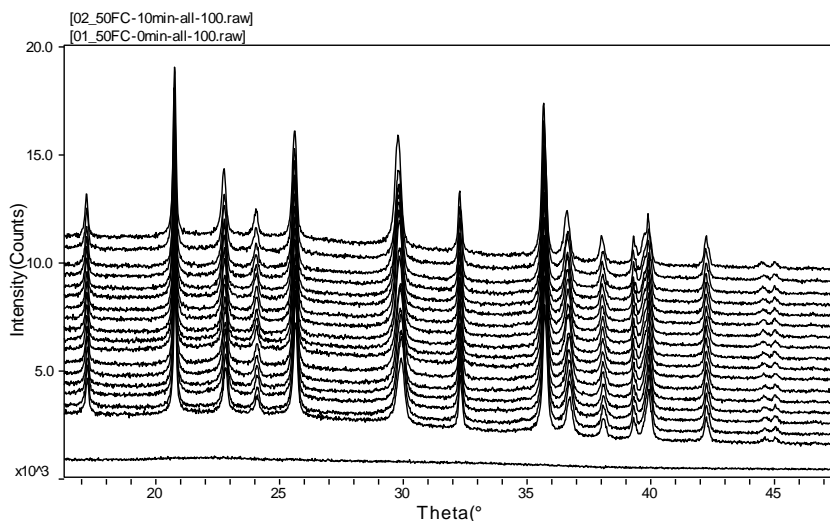

Figure 4. Group b, XRD patterns over time: 0min to 720min. Bottom to top: 0min(just reach 180°C), 10min, 20min, 30min, 40min, 50min, 60min, 80min, 100min, 120min, 150min, 180min, 210min, 240min, 360min, 480min, 600min, 720min.

To further investigate the structural changes and defects of the samples in the entire process, a more precise XRD test was performed for all the samples. The results are shown in Figure 4. The XRD patterns of the three groups exhibited a similar variation pattern; the difference is that the samples of groups A and B are in an amorphous phase at a 0-min reaction time, whereas those of group C produce a rough crystallized lithium iron phosphate, which is consistent with the SEM results. The three strong peaks of the pattern are 101 ($2\theta=20.8°$), 111 ($2\theta=25.6°$), and 311 ($2\theta=35.6°$); the fourth peak is the (020) peak. The three strong peaks stabilize with few fluctuations after 30 min of reaction and peak 020 stably increase during the first 100 min before it stabilizes. This result also indicates that 101 plane steadily grows soon after the reaction as 020 plane grows. Correspondingly, in terms of the changes in macroscopic size, lithium iron phosphate crystal tends to exhibit a stable length and width on the 020 plane, while its thickness increases, in accordance with the SEM results. To confirm the grain size of the crystal, we can calculate crystal size according to Scherrer's equation:

$$D = \frac{K\lambda}{B\cos\theta}$$

Figure 5 shows that the three groups of samples share similar characteristics. That is, within the 100-min reaction time, the thickness of 020 plane increases at the most rapid pace and stabilizes at 33 nm after 2 h. Higher concentration lead to higher initial thickness and growth speed.
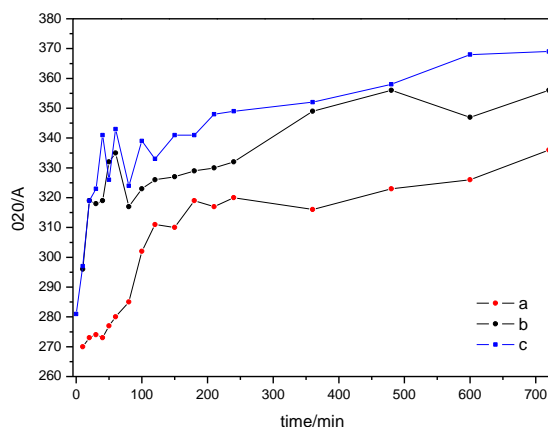

Figure 5. Three group of sample: Grain size of (020) plane

The growth of (020) plane is also related to the defect motion inside the crystal. The growth of lithium iron phosphate is a process by three-dimensional diffusion control. In such a process, the reduction of a crystal's internal defects is inevitable. Disorder is one type of point defect in the lithium iron phosphate crystal.[16,17] Various factors contribute to Fe^{2+} ion deviation from its regular position and occupy into the site of Li^+ ion, which consequently blocks the one-dimensional diffusion path of Li^+ ion. This phenomenon decreases the ionic conductance of the material and its capacity, as well as negatively affects the electrochemical performance. This kind of point defect is called the ion disorder of Fe^{2+}/Li^+.[17,18]

Quantitative research on ion disorder of Fe^{2+}/Li^+ can be achieved by the Rietveld method. Through the XRD data, verified in accordance with the Rietveld method by using the FullProf software, we can calculate the structural parameters and disorder of $Fe^{2+}/Li^{+.}$ All the XRD data were collected at a scanning speed of 2.4°/min and a step of 0.02°.[11] The refined results can be seen in Table 1 and Figure 6.

Table 1 shows that among the samples from the three groups, those with the longest reaction time exhibit a disorder of about 6%. Figure 6 illustrates the changes in the degree of synthesis with variations in reaction time; the lithium iron phosphate obtained at low concentration (group A) has a high disorder (6.91%), whereas that obtained from group B or at higher concentration has a low disorder (5.39%, 5.02%). With increasing reaction concentration, disorder tends to decrease, but group C (200%) has a double concentration of group B (100%); their disorder differs within a range of 0.5%. Furthermore, the last three samples have similar disorder. We can predict that under a sufficiently long reaction time, disorder tend to be similar. The most obvious difference is that the samples at low concentration have a higher disorder within 2-h reaction time.

Comparing the variations in thickness of (020) plane, we can see that the variations in disorder are complementary to the variations in thickness. Within 2 h, (020) plane grows the fastest as the internal disorder decreases at its fastest rate.

Table 1. disorder of three group of sample:

group	Occ Fe^{2+}	±	Fe/Li %	±	Rp	Rwp
Group a-12h	0.02965	0.0015	6.91	0.30	19.5*	15.6
Group b-12h	0.02200	0.0011	5.39	0.23	14.7	12.4
Group c-12h	0.02094	0.0011	5.02	0.23	14.9	12.4

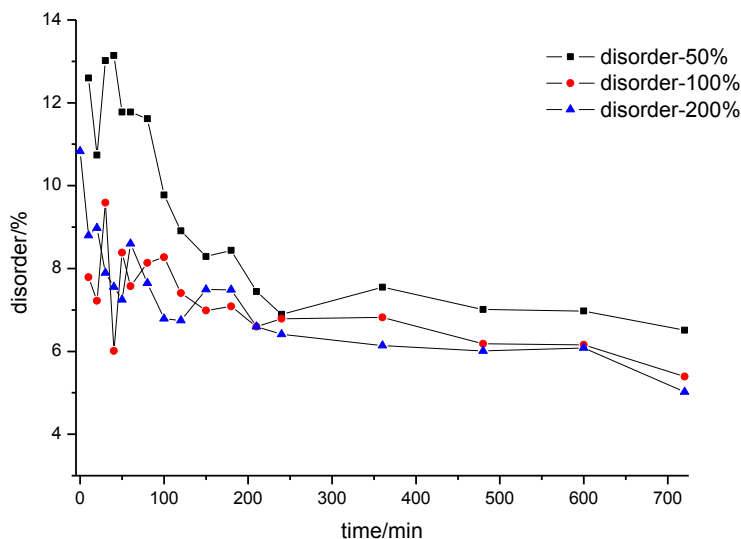*R_p and R_{wp} are calculated values. Lower, higher reliability.

Figure 6. disorder over time

The main growth process is completed within 2 h; the initial grain size at high concentration is higher and growth speed is faster with a low disorder. That is, under ordinary pressure and solvothermal conditions, the growth of lithium iron phosphate mainly takes diffusion control; reaction concentration has the most important influence on the extent of reaction. At high concentration, a small-sized lithium iron phosphate nameplates with low structural defects can be obtained more easily at a faster rate. [11,19]

4. CONCLUSIONS

In conclusion, an effective way for synthesizing $LiFePO_4$ nanoplates has been conducted. The $LiFePO_4$ nanoplates synthesized by reflux method is nano-sized, with a large exposure of (020) plane and a thickness of 30 nm. The concentration is the key factor for the reaction as the synthetic process of $LiFePO_4$ is a three-dimensional diffusion-controlled process. Higher concentration leads to stronger diffusion driving force, which benefits the crystal growth and defect motion. A low disorder nameplates crystal of $LiFePO_4$ would easily grow in such a condition. Ethylene glycol plays an important role in morphology control for this reaction. The simplicity of reflux method can provide a potential application in lithium battery industry.

References

1   H Li, Z Wang, L Chen and X Huang, *Adv. Mater.,* 45 (2009) 4593.
2   W. Zhang, *J. Power Sources,* 6 (2011) 2962.
3   S. Chung, Y. Kim and S Choi, *Adv. Funct. Mater.,* 24 (2010) 4219.
4   D. Kempaiah and H. Itaru, *Adv. Energy Mater.,* 3 (2012) 284.
5   H. Chen, A. Michel, D. Gilles, D. Franck, P. Philippe and J. Tarascon, *ChemSusChem.,* 4 (2008) 348.
6   J. Chen, S. Wang and M. Whittingham, *J. Power Sources,* 2 (2007) 442.
7   R. Malik, D. Burch, M. Bazant and G. Ceder, *Nano letters*, 10 (2010) 4123.
8   R. Pitchai, V. Thavasi, S. Mhaisalkar and S. Ramakrishna, *J. Mater. Chem.,* 30 (2011) 11040.
9   J. Chen and M. Whittingham, *Electrochem. Commun.,* 5 (2006) 855.
10 X. Qin, J. Wang, J. Xie, F. Li, L. Wen and X. Wang, *Phys. Chem. Chem. Phys.,* 8 (2012) 2669.
11 J. Chen and J. Graetz, *ACS Appl. Mater. Interfaces,* 5 (2011) 1380.
12 C. Delacourt, P. Poizot, S. Levasseur and C, Masquelier, *Electrochem. Solid St.,* 7 (2006) A352.
13 P. Axmann, C. Stinner, M. Wohlfahrt-Mehrens, A. Mauger, F. Gendron and C. Julien, *Chem. Mater.,* 8 (2009) 1636.
14 C. Nan, J. Lu, C. Chen, Q. Peng and Y. Li, *J. Mater. Chem.,* 27 (2011) 9994.

15 L. Wang, X. He, W. Sun, J. Wang, Y. Li and S. Fan*, Nano letters,* 11 (2012) 5632.
16 M. Islam, *Philosophical Transactions of the Royal Society A: Mathematical, Physical and Engineering Sciences,* 1923 (2010) 3255.
17 J. Chen, J. Bai, H. Chen and J. Graetz, *J. Phys. Chem. Lett.,* 15 (2011) 1874.
18 C. Fisher and M. Islam, *J. Mater. Chem.,* 11 (2008) 1209.
19 M. Trudeaua, D. Laulb, R. Veillettea, A. Serventia, A. Maugerc, C. Juliend and K. Zaghib, *J. Power Sources,* 18 (2011) 7383.